Chin. J. Astron. Astrophys. Vol. 6 (2006), No. 6, 680–688
(*http://www.chjaa.org*)

Chinese Journal of
Astronomy and
Astrophysics

An Efficient High-Resolution Shock-Capturing Scheme for Multi-Dimensional Flows

I. Hydrodynamics *

Cong Yu

[1] National Astronomical Observatories / Yunnan Astronomical Observatory, Chinese Academy of Sciences, Kunming 650011; *yccit@yahoo.com.cn*
[2] Graduate School of Chinese Academy of Sciences, Beijing 100049

Received 2006 February 27; accepted 2006 April 17

Abstract Many problems at the forefront of theoretical astrophysics require a treatment of dynamical fluid behavior. We present an efficient high-resolution shock-capturing hydrodynamic scheme designed to study such phenomena. We have implemented a weighted, essentially non-oscillatory (WENO) scheme to fifth order accuracy in space. HLLE approximate Riemann solver is used for the flux computation at cell interface, which does not require spectral decomposition into characteristic waves and so is computationally friendly. For time integration we apply a third order total variation diminishing (TVD) Runge-Kutta scheme. Extensive testing and comparison with schemes that require characteristic decomposition are carried out demonstrating the ability of our scheme to address challenging open questions in astrophysics.

Key words: accretion — hydrodynamics — method: numerical — shock waves

1 INTRODUCTION

High-resolution shock-capturing methods of the Godunov type have been successfully applied to various astrophysical problems in the last decade (Mellema, Eulderink & Icke 1991; Duncan & Hughes 1994; Balsara 1994; Ryu et al. 1993; Ryu & Jones 1995; Eulderink & Mellema 1995; Koide 1996; Ziegler & Yorke 1997; Komissarov 1999; Aloy et al. 1999; Font 2000; Zhang, Woosley & MacFadyen 2003; Koldoba, Kuznetsov & Ustyugova 2002), and numerical simulations with such methods have significantly enhanced our understanding of planetary nebulae, Gamma-ray bursts, astrophysical outflows and jets, physical processes of accretion disk in binaries, YSOs as well as in AGNs, the interaction of planet and protoplanetary disk, shocks in supernova remnant and dynamo processes in stars and accretion disks. Because these complex problems are generally nonlinear, there is continual demand for following the nonlinear evolution of hydrodynamic flows in such astrophysical problems.

There are several strategies for integrating the hydrodynamic equations. Nonconservative schemes, such as ZEUS (Stone & Norman 1992), have been extensively used by numerical astrophysicists, in which the internal energy rather than the total energy is followed. This is good in situations, common in astrophysics, where the internal energy is small compared to the total energy (high Mach flows). We choose to use a conservative scheme. One merit is that a total variation stable scheme is sure to converge to a weak solution of the equations by the Lax-Wendroff theorem (Lax & Wendroff 1960) and by a theorem due to LeVeque (1998). Another advantage is that a conservative scheme in any number of dimensions would satisfy the jump conditions at discontinuities. This is not the case with nonconservative schemes.

* Supported by the National Natural Science Foundation of China.

For years, high-order, conservative, upwind differencing schemes have been proven to be very efficient for solving compressible hydrodynamic equations. These methods generally depend on the estimates of mass, momentum and energy fluxes across cell interface, based on so-called Riemann problem. Examples include the Godunov scheme (Godunov 1959), the Roe scheme (Roe 1981), the total variation diminishing (TVD) scheme (Harten 1983), the PPM scheme (Colella & Woodward 1984), the BGK scheme (Xu 2000), the essentially non-oscillatory (ENO) scheme (Harten et al. 1987) and the weighted essentially non-essentially (WENO) scheme (Shu 1997). The development of these powerful methods in computational fluid dynamics has enabled us to gain deeper insights on astrophysical hydrodynamical flows. A consensus has been approached that conservative finite difference schemes based on Riemann solvers are particularly good for solving hyperbolic type system of hydrodynamic equations. Such schemes are called Godunov-type schemes, which are a class of the so-called high-resolution shock-capturing schemes (HRSC, e.g. Toro 1997; LeVeque 1992). A good hydrodynamical scheme must be able to address complex flows including strong shock interaction, and HRSC schemes of conservative type are able to satisfy the important constraint of capturing the profiles of strong discontinuities in a few numerical cells without producing spurious oscillations.

The eigenvalues and eigenvectors of the Jacobian matrices of the systems (i.e. characteristic structure of the hyperbolic system of conservation equations) are the basic building blocks of any Riemann solver. They also help people to understand physical properties of the system and to prescribe physically consistent boundary conditions. Solution to the Riemann problem in hydrodynamics has been extensively studied in the literature, and exact solutions can be reached with high order of accuracy by iterative methods (e.g. Toro 1997). However, exact Riemann solver would add extra computational cost. From this perspective, approximate solvers based on alternative strategies have been devised: local linearization, two shock approximation, flux-splitting methods, and so forth. Most of these solvers depend on expensive characteristic decompositions of the Jacobian matrix or involve iterative techniques to solve nonlinear equations.

Besides methods based on the Riemann solver, there have appeared alternative approaches based on non-oscillatory high order symmetric TVD schemes (Davis 1984; Yee 1987; Nessyahu & Tadmor 1990). These schemes are based on either Lax-Wendroff second order scheme with additional dissipation terms (Davis 1984; Roe 1984; Yee 1987) or on non-oscillatory high order extension of Lax-Friedrichs first order central scheme (Nessyahu & Tadmor 1990). The high order ENO shock capturing scheme (Harten et al. 1987) has been very successful with Euler equations. ENO type methods have been previously been implemented for computational hydrodynamics (e.g. Del Zanna & Buciantini 2002). The WENO schemes (e.g. Shu 1997) are recent extensions of ENO schemes, which take into account the information of the discarded stencils in ENO schemes.

Apart from the hydrodynamic simulation, magnetohydrodynamics and relativistic (magneto) hydrodynamics have also been extensively investigated in recent literature (e.g. Stone 1992; Ryu et al. 1995, Aloy et al. 1999; Toth 2000; De Villiers & Hawley 2003; Del Zanna 2002, for a comprehensive review see Martí & Müller 2003 and Font 2003).

This paper is structured as follows: In Section 2, we summarize the basic fluid equations. We give a basic description of the algorithms in Section 3. Finally in Section 4, we discuss various tests and applications of our efficient shock-capturing scheme.

2 EULER EQUATION AND THE EIGENSYSTEM

We will consider multi-dimensional problems in this paper, and confine our discussion to two dimensional problems for simplicity. Extension to three dimensions is straightforward. The two dimensional Euler equation reads

$$\frac{\partial U}{\partial t} + \frac{\partial F(U)}{\partial x} + \frac{\partial G(U)}{\partial y} = 0 \,, \tag{1}$$

where $U = (\rho, \rho u, \rho v, \rho E)^T$, $F(U) = (\rho u, \rho u^2 + p, \rho uv, (\rho E + p)u)^T$, $G(U) = (\rho v, \rho uv, \rho v^2 + p, (\rho E + p)v)^T$, and $p = (\gamma - 1)\rho e$, $E = e + \frac{1}{2}(u^2 + v^2)$.

We have two Jacobi matrixes, $A = \partial F(U)/\partial U$ and $B = \partial G(U)/\partial U$.

The right eigenvectors of matrix A are

$$R_1 = \begin{pmatrix} 1 \\ u-c \\ v \\ H-uc \end{pmatrix} \quad R_2 = \begin{pmatrix} 0 \\ 0 \\ 1 \\ v \end{pmatrix} \quad R_3 = \begin{pmatrix} 1 \\ u \\ v \\ \frac{1}{2}(u^2+v^2) \end{pmatrix} \quad R_4 = \begin{pmatrix} 1 \\ u+c \\ v \\ H+uc \end{pmatrix} . \tag{2}$$

The eigenvalues of matrix A are $u-c$, u, u and $u+c$. The right eigenvectors of matrix B have a similar form with eigenvalues $v-c$, v, v and $v+c$.

A conservative scheme updates a set of conserved variables at each time step. Our vector of conservative variables is $U = (\rho, \rho u, \rho v, \rho E)^T$. The vector of primitive variables is $V = (\rho, u, v, p)^T$, which is used for the following discussion on spatial reconstructions. The relation of p and ρE is $\rho E = p/(\gamma-1) + \frac{1}{2}\rho(u^2 + v^2)$. In Newtonian cases, the relation between the conservative and primitive variables is straightforward. In relativistic cases, however, it would become much more complex and be a crucial part for the success of numerical integration (Gammie et al. 2003).

3 THE ALGORITHM OF HIGH-RESOLUTION SHOCK-CAPTURING SCHEME

3.1 WENO Spatial Reconstruction

Our scheme follows closely the prescriptions of the WENO reconstruction devised by Shu (1997). Here we give a brief, self-contained description of this interpolation method. We choose the reconstruction based on primitive variables which has the advantage of keeping the positivity of pressure (see Mignone et al. 2005). Let v represent any one component of primitive variable $V = (\rho, u, v, p)^T$,

$$v^{(r)-}_{i+\frac{1}{2}} = \sum_{j=0}^{k-1} c_{rj} v_{i-r+j} , \qquad v^{(r)+}_{i-\frac{1}{2}} = \sum_{j=0}^{k-1} \widetilde{c}_{rj} v_{i-r+j} , \tag{3}$$

where $v^{(r)-}_{i+\frac{1}{2}}$ $(r = 0, 1, ..., k-1)$ stands for rth linear combination of v_{i-r+j}, with combination coefficients c_{rj}. Similarly, $v^{(r)+}_{i-\frac{1}{2}}$ $(r = 0, 1, ..., k-1)$ stands for the rth linear combination of v_{i-r+j}, with combination coefficients $\widetilde{c}_{rj}$. Note here $\widetilde{c}_{rj} = c_{r-1,j}$. The values of c_{rj} for the case of $k = 3$ are give in Tabel 1.

Table 1 Values of c_{rj} for the case of $k = 3$

k	r	$j=0$	$j=1$	$j=2$
3	–1	11/6	–7/6	1/3
3	0	1/3	5/6	–1/6
3	1	–1/6	5/6	1/3
3	2	1/3	–7/6	11/6

The actual value of $v^-_{i+\frac{1}{2}}$ is a weighted sum of $v^{(r)-}_{i+\frac{1}{2}}$ with weights ω_r. We may apply a similar procedure to $v^{(r)+}_{i-\frac{1}{2}}$ to obtain the value of $v^+_{i-\frac{1}{2}}$ with weights $\widetilde{\omega}_r$,

$$v^-_{i+\frac{1}{2}} = \sum_{r=0}^{k=1} \omega_r v^{(r)-}_{i+\frac{1}{2}} , \qquad v^+_{i-\frac{1}{2}} = \sum_{r=0}^{k=1} \widetilde{\omega}_r v^{(r)+}_{i-\frac{1}{2}} . \tag{4}$$

For the case of $k = 3$, the weights ω_r and $\widetilde{\omega}_r$ are defined as

$$\omega_r = \frac{\alpha_r}{\sum_{s=0}^{k-1} \alpha_s}, \quad \alpha_r = \frac{d_r}{(\epsilon + \beta_r)^2}, \quad r = 0, \ldots, k-1 , \tag{5}$$

$$\widetilde{\omega}_r = \frac{\widetilde{\alpha}_r}{\sum_{s=0}^{k-1} \alpha_s}, \quad \widetilde{\alpha}_r = \frac{\widetilde{d}_r}{(\epsilon + \beta_r)^2}, \quad r = 0, \ldots, k-1 , \tag{6}$$

where

$$d_0 = 0.3\,, \quad d_1 = 0.6\,, \quad d_2 = 0.1\,, \tag{7}$$

$$\widetilde{d}_r = d_{k-1-r}, \quad r = 0, \ldots, k-1\,, \tag{8}$$

and

$$\beta_0 = \frac{13}{12}(v_i - 2v_{i+1} + v_{i+2})^2 + \frac{1}{4}(3v_i - 4v_{i+1} + v_{i+2})^2\,, \tag{9}$$

$$\beta_1 = \frac{13}{12}(v_{i-1} - 2v_i + v_{i+1})^2 + \frac{1}{4}(v_{i-1} - v_{i+1})^2\,, \tag{10}$$

$$\beta_2 = \frac{13}{12}(v_{i-2} - 2v_{i-1} + v_i)^2 + \frac{1}{4}(v_{i-2} - 4v_{i-1} + 3v_i)^2\,. \tag{11}$$

Following the above spatial reconstruction procedures, we can acquire the primitive variable values $\rho^-_{i+\frac{1}{2}}$, $\rho^+_{i+\frac{1}{2}}$, etc., at the cell interface $x_{i+\frac{1}{2}}$. From the primitive variables we obtain fluxes such as the mass fluxes $(\rho u)^-_{i+\frac{1}{2}}$, $(\rho u)^+_{i+\frac{1}{2}}$, at the cell interface $x_{i+\frac{1}{2}}$. We then construct numerical fluxes $\overline{F}_{i+\frac{1}{2}}$ =HLLE$(F^-_{i+\frac{1}{2}}, F^+_{i+\frac{1}{2}})$ in terms of the left and right fluxes (HLLE stands for the HLLE approximate Riemann Solver). The construction of numerical fluxes depends on which Riemann Solver is applied, this will be discussed in next section. According to the known fluxes, we update the conservative variables in the x direction using the TVD Runge-Kutta time integration to get $\mathcal{L}_x(U^n)$ (for the detailed expression of $\mathcal{L}_x(U^n)$, see Eqs. (18)–(20) in Section 3.3). The multidimensional integration is obtained by directionally split method with Strang splitting (Strang 1968). Let $\mathcal{L}_x(U)$ and $\mathcal{L}_y(U)$ denote the one dimensional operators in the x and y directions, respectively, the solution at time $t = t^n$ is then updated at every other step:

$$U^{n+2} = \mathcal{L}_x\mathcal{L}_y\mathcal{L}_y\mathcal{L}_x(U^n)\,. \tag{12}$$

3.2 Approximate Riemann Problem Solver

In 1959, Godunov presented a first order upwind scheme which could capture shock waves without introducing spurious oscillations. Godunov's method and its various derivatives have since gained increasing popularity due to their robustness and ability to achieve high-resolution of discontinuities. From then on, various approximate Riemann Problem Solvers have appeared in the literature. Typical ones include: 1) Nonlinear exact Riemann Solver; 2) Roe type approximate Riemann Solver; 3) BGK type Riemann Solver; 4) HLLE type Riemann Solver; 5) Marquina's Riemann Solver; 6) Flux splitting Riemann Solver. At the cell interface, a local Riemann problem has to be solved, which can be effectively done with a nonlinear iterative method. However, this is very expensive. The Roe type linearized Riemann solver is to define an average state at the cell interface and it requires characteristic decompositions to compute the fluxes at the cell interface.

Here we would choose the most easily implemented approximate yet diffusive approximate Riemann Solver, that of the HLLE type. Another reason of our choice is that this solver is the most computationally friendly. In this solver, we need only the maximum propagation speed (i.e. maximum eigenvalue of Jacobi matrix), and the characteristic decomposition is avoided, greatly reducing the computation costs. In this Riemann Solver, shocks are resolved properly but the contact discontinuity (corresponding to middle eigenvalue u) would be somewhat smeared. The HLLE (Harten, Lax & van Leer 1983; Einfeldt 1988; Einfeldt et al. 1991) approximate Riemann Solver is defined as follows:

$$\overline{F}(U_R, U_L) = \frac{\alpha^+ F(U_L) - \alpha^- F(U_R) + \alpha^+\alpha^-(U_R - U_L)}{\alpha^+ - \alpha^-}, \tag{13}$$

$$\alpha^+ = \max\{0, \alpha_R\}, \quad \alpha^- = \min\{0, \alpha_L\}. \tag{14}$$

Einfeldt (1991) proposed that α_L and α_R should take the form

$$\alpha_L = \min\{\bar{u} - \bar{c}, u_L - c_L\}, \quad \alpha_R = \max\{\bar{u} + \bar{c}, u_R - c_R\}, \tag{15}$$

where $\bar{u}$ and $\bar{c}$ are Roe average of left and right states at the cell interface,

$$\bar{u} = \frac{\sqrt{\rho_L} * u_L + \sqrt{\rho_R} * u_R}{\sqrt{\rho_L} + \sqrt{\rho_R}}, \qquad \bar{v} = \frac{\sqrt{\rho_L} * v_L + \sqrt{\rho_R} * v_R}{\sqrt{\rho_L} + \sqrt{\rho_R}}, \tag{16}$$

$$\bar{h} = \frac{\sqrt{\rho_L} * h_L + \sqrt{\rho_R} * h_R}{\sqrt{\rho_L} + \sqrt{\rho_R}}, \qquad \bar{c} = \left\{(\gamma - 1)\left[\bar{h} - \frac{1}{2}(\bar{u}^2 + \bar{v}^2)\right]\right\}^{1/2}. \tag{17}$$

If $\alpha^+ = \alpha^-$, the HLLE flux becomes the so-called local Lax-Friedrichs flux.

3.3 Runge-Kutta TVD Time Integration

In order to achieve high order accuracy in time, the time integration is done using a high order TVD Runge-Kutta scheme (Shu & Osher 1988), which combines the first order Euler steps and involves prediction and correction. For example, the third order accuracy in x direction is achieved by

$$U^{(1)} = U^n + \Delta t \mathcal{H}\left(U^n\right), \tag{18}$$

$$U^{(2)} = \frac{3}{4}U^n + \frac{1}{4}U^{(1)} + \frac{1}{4}\Delta t \mathcal{H}\left(U^{(1)}\right), \tag{19}$$

$$\mathcal{L}_x(U^n) = \frac{1}{3}U^n + \frac{2}{3}U^{(2)} + \frac{2}{3}\Delta t \mathcal{H}\left(U^{(2)}\right), \tag{20}$$

where $\mathcal{H}$ is an operator and $\mathcal{H}(U^n) = \frac{1}{\Delta x}(\overline{F}_{i+\frac{1}{2}} - \overline{F}_{i-\frac{1}{2}})$. Similarly in the definition of $\mathcal{L}_y(U^n)$ in the y-direction, the operator $\mathcal{H}$ should be defined by $\mathcal{H}(U^n) = \frac{1}{\Delta y}(\overline{G}_{i+\frac{1}{2}} - \overline{G}_{i-\frac{1}{2}})$. Our explicit scheme is subject to the Courant-Friedrich-Levy (CFL) condition. For two dimensional problem, the time step is determined by

$$\Delta t = C_{\mathrm{CFL}} \times \min\left[\frac{\Delta x}{\max(|u| + c)}, \quad \frac{\Delta y}{\max(|v| + c)}\right].$$

We usually choose a CFL number, C_{CFL}, between 0.5–0.8.

To summarize, this is a high-resolution conservative (shock-capturing) scheme based on accurate fifth order reconstruction WENO-type algorithms and on an approximate Riemann Solver flux formula (HLLE) which does not involve time-consuming characteristic decomposition. The scheme is simple and efficient, since complex Riemann problem solver based on characteristic wave decomposition is avoided: the solver is defined by the two fastest local wave speeds and the spatial reconstruction at cell boundaries is achieved by using WENO-type interpolating method.

4 NUMERICAL TESTS AND ASTROPHYSICAL APPLICATIONS

In this section we shall give extensive examples to illustrate the application of our scheme and compare our scheme with schemes that require characteristic decomposition. For the latter we chose the Roe Riemann Solver (Roe 1981), which is a typical Riemann Solver and needs characteristic decomposition. Because characteristic decomposition would cost additional computation time, we use relatively simple MUSCL spatial reconstruction (van Leer 1979). In the WENO+HLLE calculation, the calculation of the smooth indicator takes most of the computing time. In the MUSCL+ROE scheme, the computation cost of spatial reconstruction is smaller than in the WENO+HLLE, but it needs additionally characteristic decomposition. On the whole the two methods have comparable computation costs.

We investigate the decomposition of initial discontinuity into three elementary waves: a shock, a contact discontinuity and a rarefaction wave. For such simple problems in one dimension, an analytical solution can be found (see Toro 1997). Due to their relative simplicity, one dimensional problems are also excellent benchmarks that can be used for comparison of different algorithms and implementations. Finally, we consider an astrophysical application: binary accretion flow.

4.1 One Dimensional Shock Tube Problems

These are standard problems for testing codes for shock calculations. In the one dimensional shock tube a thin membrane initially separates two static gas states characterized by different parameters. At $t = 0$ the membrane is broken and the two gases begin to interact. The state to the left of the membrane is $(\rho, u, p)^L = (1, 0, 1)$ and the state on the other side is $(\rho, u, p)^R = (0.125, 0, 0.1)$, where the superscript L stands for the initial condition $0 \leq x \leq 0.5$ and R, $0.5 \leq x \leq 1.0$. A rarefaction wave develops and propagates to the left while the contact discontinuity separating the two gases and the shock wave are both moving to the right.

In Figure 1 we compare our scheme with MUSCL scheme (van Leer 1979) plus Roe Riemann Solver (Roe 1981), which requires characteristic decomposition. The cell number in both calculations is 800 and the final time is $t = 0.2$.

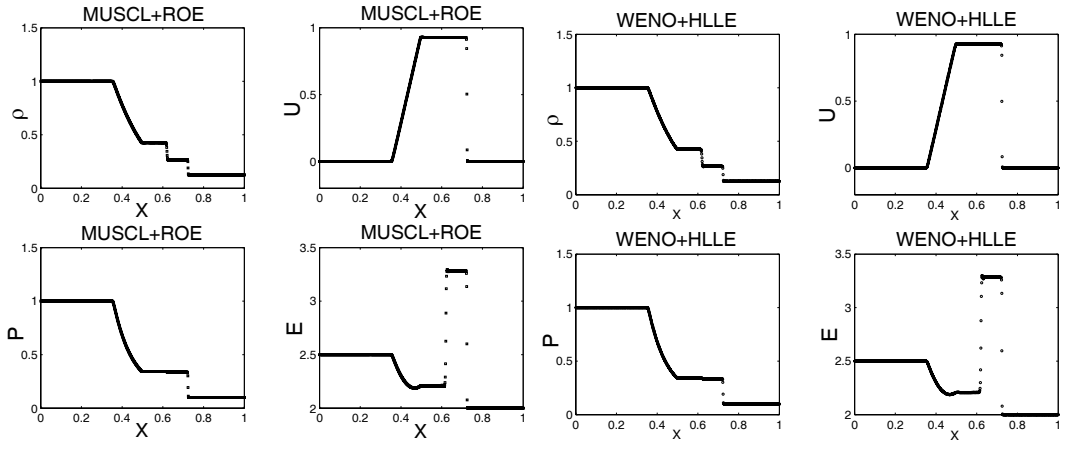

Fig. 1 Solutions of the shock tube problem with MUSCL+ROE (left panels) and with WENO+HLLE (right panels). Final time is $t = 0.2$. For this simple problem the two schemes achieve comparable resolution. The shocks are resolved by about three cells and the CDs are resolved by about six cells.

We see that, in this simple example, there is no obvious differences between the two schemes: they achieve almost the same resolution at the shock (about three celss) and at the contact discontinuities (about six cells). However, if we carried out the calculation without WENO spatial reconstruction, then the shock position would have been resolved with about nine cells and the CDs, over 25 cells. From this example we could see even if we use the most readily implemented HLLE Riemann solver, we have a satisfactory resolution only when we use the high order WENO spatial reconstruction method, which offsets the disadvantage of the HLLE Riemann solver.

4.2 Two Dimensional Riemann Problems

Two dimensional Riemann problems were widely studied by various authors to check their numerical schemes (e.g. Lax & Liu 1998). This problem involves the interactions of four initially independent constant states in a two-dimensional plane. The interaction of the four states would produce very complicated pattern as a result of interaction of shock, rarefaction and contact discontinuity. We calculate the configurations labelled 5 and 12 in Lax & Liu (1998). We refer the readers to Lax & Liu (1998) for the detailed initial conditions. The left four panels of Figure 2 compare the solutions produced by the two schemes for the configuration 5; the right four panels, for the configuration 12. The lower panels of Figure 2 give the density profile along a diagonal cut in the corresponding upper panel. We can see that the results of WENO+HLLE are a bit better than that of MUSCL+ROE: WENO+HLLE requires fewer cells to resolve the discontinuities than does MUSCL+ROE.

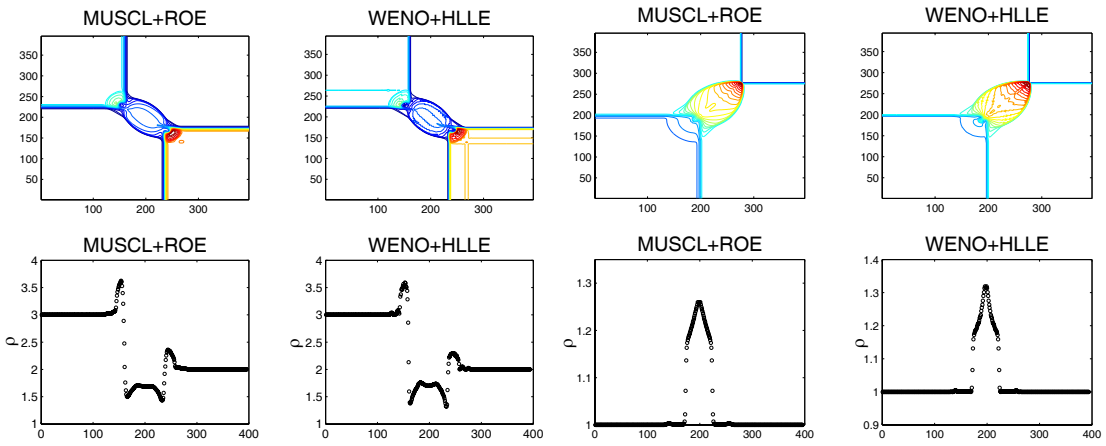

Fig. 2 Upper panels show the density contours of a 2D Riemann problem obtained by the two schemes, WENO+HLLE and MUSCL+ROE, for configuration 5 (left panels) and for configuration 12 (right panels). The lower panels show the density profile along a diagonal cut in the corresponding upper panel. This figure shows that WENO+HLLE can resolve the discontinuities better than MUSCL+ROE.

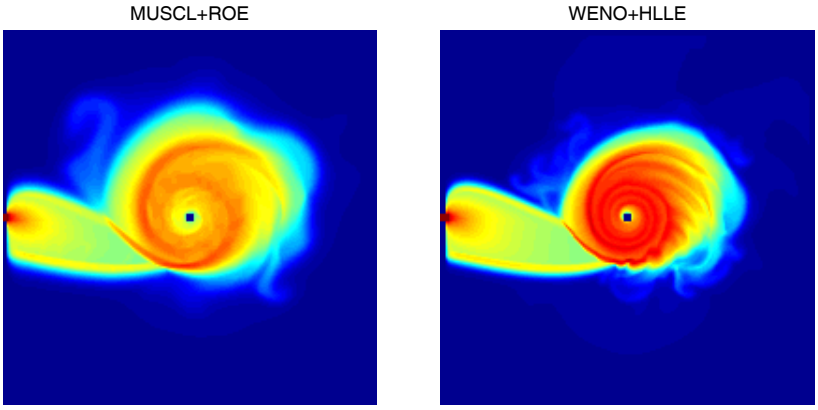

Fig. 3 2D density solutions of binary accretion flow with a logarithmic scale after eight periods of revolution computed with MUSCL+ROE (left) and WENO+HLLE (right).

4.3 Multidimensional Astrophysical Applications

Hydrodynamics is expected to play a significant role in many phenomena typical in astrophysics. In this section we present the results of application of our algorithm to the problem of binary accretion flow. The basic setup of this problem is taken from Makita et al. (2000), who use an AUSM (advection upwind splitting method) type scheme to solve the problem. To be self-contained, we briefly describe the problem here. The binary system is composed of a mass-accreting primary with mass M_1 and a mass-losing secondary with M_2. The mass ratio is defined as $q = M_2/M_1$. The basic equations are two dimensional inviscid Euler equations. Following Makita et al. (2000), we add source terms $\rho\kappa_x$, $\rho\kappa_y$ and $\rho(u\kappa_x + v\kappa_y)$ to the momentum equations and energy equation, respectively. Detailed expressions of κ_x and κ_y are given by the equations (3) and (4) in Makita et al. (2000). As an initial condition, we suppose that the whole computational region, $-0.5 \leq x, y \leq 0.5$, is filled with a tenuous gas, with $\rho_0 = 10^{-5}, p_0 = 10^{-4}/\gamma$ and $u_0 = 0, v_0 = 0$. This initial condition is also maintained outside of the outer boundary except for the L1

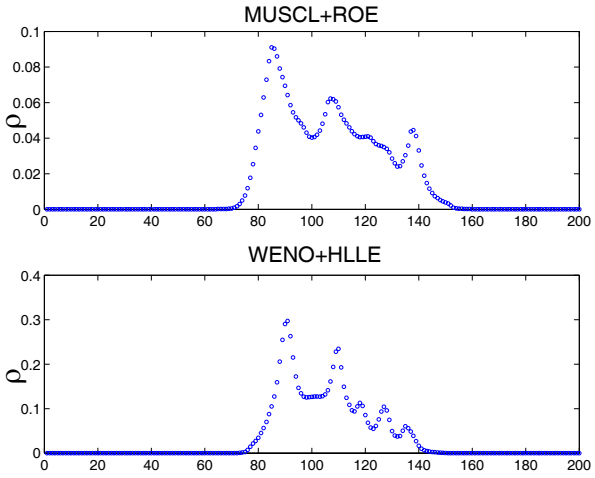

Fig. 4 Density profiles along $x = 0.1$ in Fig. 3 calculated by MUSCL+ROE and WENO+HLLE.

point and inside of the inner boundary. A small rectangular inlet hole is placed at the L1 point. The values at the inlet are $\rho_{\rm in} = 1.0, p_{\rm in} = 10^{-2}/\gamma, u_{\rm in} = 0.01$ and $v_{\rm in} = 0$ throughout the whole evolution. The mass flux from the L1 point is computed by solving a Riemann problem. The mass-accreting star is represented by a hole of 3×3 cells. In Figure 3, we show the density solutions of this binary accretion problem, and in Figure 4 we plot the density distribution at $x = 0.1$. Similar to the previous problems, we can obtain more delicate structures with the WENO+HLLE calculation, in the sense that the ability to resolve shocks and discontinuities is better in WENO+HLLE than in MUSCL+ROE. Even though characteristic decomposition is not used in WENO+HLLE, its resolution is satisfactory due to its high order spatial reconstruction.

We also carried out calculations on Kelvin-Helmholtz instability, Rayleigh-Taylor instability as well as axisymmetric jet propagation problem using our scheme. The results show that our scheme can achieve better resolutions compared with MUSCL+ROE scheme in all these problems.

5 CONCLUSIONS AND FUTURE WORK

In this paper we give an efficient numerical scheme for astrophysical dynamical problems, by coupling the WENO scheme (Shu 1997) with a simple and efficient approximate Riemann HLLE solver. The scheme has the advantage of dispensing with spectral decomposition. We have applied this efficient high-resolution shock-capturing scheme to a variety of problems containing both discontinuities and complex structures.

For many problems containing only simple shocks with almost linear smooth solutions in between, such as most Riemann problems (shock tube problems), a good second order method, such as the MUSCL methods, would be the best choice. However, when the solution contains both discontinuities and complex solution structures in the smooth regions, a higher order method would be preferable. From a comparison of the HLLE solver and the ROE solver that requires characteristic decomposition, we conclude that a high order spatial reconstruction could offset the disadvantage of HLLE Riemann solver and provide satisfactory results. An extension of the current numerical scheme to relativistic hydrodynamic and magnetohydrodynamic problems is being developed and will be discussed in separate papers.

Acknowledgements The author thanks the anonymous referee for suggestions and comments that further improved this paper. This work was funded by the National Natural Science Foundation of China (NSFC, G10533050).

References

Balsara D. S., 1994, J. Comput. Phys., 114, 284
Colella P., Woodward P. R., 1984, J. Comput. Phys., 54, 174
Colella P., 1990, J. Comput. Phys., 87, 171
Davis S. F., 1984, ICASE report 84-20, NASA Langley Research Center, VA
Del Zanna L., Bucciantini N., 2002, A&A, 390, 1177
Duncan G. C., Hughes P. A., 1994, ApJL, 436, 119
Einfeldt B., 1988, SIAM J. Numer. Anal. 25, 294
Einfeldt B., Munz C D., Roe P. L. et al., 1991, J. Comput. Phys., 92, 273
Eulderink F., Mellema G., 1995, A&AS, 110, 587
Font J. A., 2003, Living Rev. Relativity, 6, 4
Gammie C. F., McKinney J. C., Tóth G., 2003, ApJ, 589, 444
Godunov S. K., 1959, Math. Sb., 47, 271
Harten A., 1983, J. Comput. Phys., 49, 357
Harten A., Engquist B., Osher S. et al., 1987, J. Comput. Phys., 71, 231
De Villiers J. P., Hawley J. F., 2003, ApJ, 589, 458
Koldoba A. V., Kuznetsov O. A., Ustyugova G. V., 2002, MNRAS, 333, 932
Komissarov S. S., 1999, MNRAS, 303, 343
Lax P. D., Liu X.-D., 1998, SIAM J. Sci. Comput., 19, 319
Lax P. D., Wendroff B., 1960, Commun. Pure Appl. Math., 13, 217
LeVeque R. J., 1992, Numerical Methods for Conservation Laws, Basel: Birkhauser-Verlag
LeVeque R. J., 1998, In: O. Steiner and A. Gautschy, eds., Computational Methods for Astrophysical Fluid Flow, Berlin: Springer, 1
Makita M., Miyawaki K., Matsuda T., 2000, MNRAS, 316, 906
Marquina A., Martí J. M., Ibáñez J. M., Miralles J. A., Donat R., 1992, A&A, 258, 566
Martí J. M., Müller E., 2003, Living Rev. Relativity, 6, 7
Mellema G., Eulderink F., Icke V., 1991, A&A, 252, 718
Miller G. H., Colella P., 2001, J. Comput. Phys., 167, 131
Mignone A., Massaglia S., Bodo G., 2004, Ap&SS, 293, 199
Mignone A., Plewa T., Bodo G., 2005, ApJS, 160, 199
Nessyahu H., Tadmor E., 1990, J. Comput. Phys., 87, 408
Roe P. L., 1981, J. Comput. Phys., 43, 357
Ryu D., Ostriker J. P., Kang H., Cen R., 1993, ApJ, 414, 1
Ryu D., Jones T. W., 1995, ApJ, 442, 228
Saltzman J., 1994, J. Comput. Phys., 115, 153
Shu C. W., Osher S., 1988, J. Comput. Phys., 77, 439
Shu C. W., 1997, ICASE Rep. 97-65, NASA Langley Research Center, VA
Strang G., 1968, SIAM J. Numer. Anal. 5. 506
Stone J. M., Norman M. L., 1992, ApJS, 80, 753
Toro E. F. 1997, Riemann Solvers and Numerical Methods for Fluid Dynamics, Berlin: Springer-Verlag
Tóth G., 1996, Astrophysical Letters & Communication, 34, 245
Van Leer B., 1979, J. Comput. Phys., 32, 101
Xu K., 2001, J. Comput. Phys., 171, 289
Yee H. C., 1987, J. Comput. Phys., 68, 151
Ziegler U., Yorke H. W., 1997, Comp. Phys. Comm., 101, 54